Soil Biology and Biochemistry 192 (2024) 109395

Contents lists available at ScienceDirect

Soil Biology and Biochemistry

journal homepage: www.elsevier.com/locate/soilbio

Microbial mediation of soil carbon loss at the potential climax of alpine grassland under warming

Zhengxiong Liang [a], Xue Guo [b,*], Suo Liu [a], Yifan Su [a], Yufei Zeng [a], Changyi Xie [a], Qun Gao [a], Jiesi Lei [a], Baochan Li [a], Mei Wang [c], Tianjiao Dai [a,d], Liyuan Ma [e], Fenliang Fan [f], Yunfeng Yang [a], Xuehua Liu [a], Jizhong Zhou [g,h,i]

[a] State Key Joint Laboratory of Environment Simulation and Pollution Control, School of Environment, Tsinghua University, Beijing, China
[b] State Key Laboratory of Urban and Regional Ecology, Research Center for Eco-Environmental Sciences, Chinese Academy of Sciences, Beijing, China
[c] School of Geographical Sciences, South China Normal University, Guangzhou, China
[d] School of Water Resources and Environment, China University of Geosciences, Beijing, China
[e] School of Environmental Studies, China University of Geosciences, Wuhan, China
[f] Key Laboratory of Plant Nutrition and Fertilizer, Ministry of Agriculture, Institute of Agricultural Resources and Regional Planning, Chinese Academy of Agricultural Sciences, Beijing, China
[g] Institute for Environmental Genomics, University of Oklahoma, Norman, OK, USA
[h] Department of Microbiology and Plant Biology, University of Oklahoma, Norman, OK, USA
[i] Earth and Environmental Sciences Division, Lawrence Berkeley National Laboratory, Berkeley, CA, USA

ARTICLE INFO

Keywords:
Climate warming
Climax
Soil organic carbon
Microbial community
Cold regions

ABSTRACT

Soil in high latitude and altitude cold regions contains over half of soil organic carbon (SOC) globally, so the decomposition of these SOCs under climate warming could release huge amounts of carbon dioxide to the atmosphere, amplifying climate warming. However, it is still unclear how the SOC storages will change when the ecosystem reaches the final and stable stage (i.e., the climax) under long-term warming. This is mainly because the turnover times of SOC in cold regions exceeds hundreds or even thousands of years, much longer than the periods of simulated warming experiments. Herein we used natural geothermal warming gradients in a Tibetan alpine grassland to determine SOC changes and underlying plant and microbial mechanisms at the potential climax. SOC concentrations were significantly decreased by 21.4%–30.6% under high-level soil warming (+4~+6 °C), but remained unchanged under low-level soil warming (+2 °C). The losses of SOC were primarily from mineral-associated organic carbon, rather than unprotected particulate organic carbon. The shifts of microbial communities and associated decline of microbial carbon use efficiency, rather than plant-driven carbon fluxes, substantially contributed to the SOC changes. This observed SOC losses at the climax of alpine grassland by high-level warming provide strong empirical support for the positive soil carbon-climate feedback in cold regions, which could not be concluded from short-term experiments or only based on ecosystem carbon fluxes alone. The divergent responses of SOC to different degrees of warming suggest that models must account for these heterogeneous carbon dynamics for projecting future climate warming scenarios.

1. Introduction

Soil stores vast quantities of organic carbon, with roughly 1100–1700 Gt of SOC in high latitude and altitude cold regions (i.e., the Tibetan Plateau alpine grassland and Arctic tundra) (Schmidt et al., 2011; Hugelius et al., 2014; de Vrese and Brovkin, 2021). Thus, even small losses from these SOC stocks would result in significant increases in atmospheric carbon dioxide concentrations, further intensifying global climate warming (Heimann and Reichstein, 2008). In recent decades, intensive studies document warming effects on soil carbon and associated plant and microbial mechanisms. Generally, warming could increase soil carbon inputs by alleviating enzymatic limits on photosynthesis (Reich et al., 2018), enhancing plant productivity, and promoting root depth (Y. Wu et al., 2021; Zhang et al., 2016). However, warming could also increase evapotranspiration and decrease soil moisture, thus slowing down the growth of plants and limiting

* Corresponding author.
E-mail address: xueguo@rcees.ac.cn (X. Guo).

https://doi.org/10.1016/j.soilbio.2024.109395
Received 28 May 2023; Received in revised form 6 March 2024; Accepted 8 March 2024
Available online 9 March 2024

plant-derived carbon in the soil (Li et al., 2018). The different responses of plants to warming might be depended on multiple factors based on the multiple limitation theory (Reich et al., 2018). Meanwhile, soil microbial community is also a crucial factor influencing soil carbon cycling and could respond diversely to climate warming (Liu et al., 2019). Some studies indicate that warming could stimulate SOC decomposition and microbial respiration (Meng et al., 2020), while others suggest that warming might reduce soil moisture supply, thereby inhibiting microbial respiration (Fang et al., 2018) and enzyme activity (Garcia-Palacios et al., 2018). The contrasting responses of microbial-mediated carbon cycling processes to warming contribute to significant uncertainties in predicting the impacts of climate warming on soil carbon storages (Hararuk et al., 2015).

Until now, whether climate warming results in a net SOC loss remains uncertain (Todd-Brown et al., 2018; van Gestel et al., 2018). Recently, a study reported that two decades of warming led to significant losses of surface soil carbon in an alpine ecosystem possibly due to warming inhibiting microbial pathways to soil carbon formation and/or stimulate microbial use of heavy fraction carbon (Chen et al., 2023). However, a meta-analysis of 74 warming experiments ranging from 5 years to 20 years indicated that warming had a minor effect on surface soil organic carbon in alpine ecosystems on the Tibetan Plateau (Chen et al., 2022b). Such uncertainty may have been partly due to that the durations of most experimental studies are still much shorter than soil carbon turnover times, especially in high latitude and altitude cold regions.

In most ecosystems, soil carbon turnover times vary from decades to hundred years, which are dependent on the combined effects of vegetation type, climate, soil and land use (Erb et al., 2016; He et al., 2016; Wang et al., 2018). Due to low temperatures which constrain microbial SOC mineralization in cold regions, soil carbon turnover times could be more than 500 years in the Tibetan Plateau alpine grassland and Arctic tundra (Wu et al., 2021). Given that most warming manipulation experiments limit their durations to one or two decades (Crowther et al., 2016), the observed effects of warming on SOC in these cold regions are likely in the initial stage rather than in the final and stable stage (i.e., the potential climax). Definitely, it will lead to great uncertainties when future changes in SOC were projected by only using these short-term observations. Therefore, there is a great need to conduct longer-term warming studies in these cold regions in order to better understand SOC change at the potential climax after long enough periods of warming.

Cold regions in high latitudes and altitudes have experienced more rapid climate warming, whose rate is more than twice the global average in the past 50 years (Chen et al., 2013; Cohen et al., 2014; Jia et al., 2017). Therefore, 21st-century warming in these regions could exceed 3–4 °C with a high probability, even if Paris Agreement 1.5 or 2 °C goals could be met. However, due to energy supply limitation in high latitude and altitude cold regions, most *in situ* warming experiments only have been designed to impose low levels of warming (1–2 °C) to test ecosystem responses (Zhou et al., 2012; Collins et al., 2021; Qi et al., 2021; Chen et al., 2022b). Low- and high-levels of warming can divergently alter soil temperature, water content, nutrient availability, and vegetation coverage and composition, which may result in different changes of soil carbon cycling (Wang et al., 2020, 2021). A short-term warming experiment documented that 2 °C warming didn't alter the carbon sequestration capacity of alpine grassland, but 4 °C warming significantly shifted the ecosystem from a net carbon sink to a net carbon source (Zhu et al., 2016). However, how different warming levels affect SOC in longer periods of time is still poorly understood. Evidence for how SOC in cold regions shifts under different warming levels would identify possible tipping points of ecosystem response to climate warming. A deeper understanding and quantification of SOC changes in response to varying warming levels would therefore be needed to accurately predict future climate warming scenarios.

One possibility to study the final and stable stage of SOC in cold regions with large warming gradients is to use ecosystems affected by natural geothermal activity (Sigurdsson et al., 2016). In this study, we used an *in situ* natural warming study in Qinghai-Tibetan Plateau to determine the SOC changes and underlying plant and microbial mechanisms. The study exploits geothermal hot springs (100°32′26″ E, 37°9′1″ N; 3436 m above sea level) in an alpine grassland that have soil temperature gradients from ambient temperature to +6 °C (Supplementary Figs. 1a–c). The warming gradients around the hot springs are confined to a small area (i.e., radius <25 m), and thus are free of the usual confounding effects of biogeographical variations or other environmental gradients (O'Gorman et al., 2014; O'Gorman et al., 2017). According to local legends and historical records (Li and Wang, 1994), these geothermal hot springs have been present stably for at least one thousand years, which is confirmed by soil ^{14}C age estimation. It provides a unique platform for assessing SOC at the potential climax under warming in the cold regions that hold large carbon storages (Intergovernmental Panel on Climate, 2014). Here we took soil samples (0–15 cm) from ambient, +2 °C, +4 °C and +6 °C warmed plots along the warming gradients around the geothermal hot springs in 2020 and 2021 (Supplementary Fig. 1c). Our results revealed that high-level warming significantly decreased SOC especially for mineral-associated organic carbon (MAOC), which was substantially due to the shifts of microbial communities and associated decline of microbial carbon use efficiency under high levels of warming.

2. Materials and methods

2.1. Site description and sampling

The study site is located in a typical alpine grassland ecosystem of the Qinghai-Tibet Plateau in China at 3436 m above sea level (100°32′26″ E, 37°9′1″ N). This cold region has a continental monsoon climate with a mean annual precipitation of 389 mm and a mean annual temperature of 0.1 °C, according to the climatological survey data from 1981 to 2010 of the closest (<20 km away) synoptic station in Gangcha County, Qinghai, China (http://www.nmic.cn/). The alpine grassland is dominated by *Kobresia humilis*, *Astragalus tanguticus*, *Potentilla pamiroalaica*, and *Plantago major*. Geothermal hot springs cause stable temperature gradients in the surrounding soil ranging from ambient temperature (mean August temperature from 2020 to 2021: 14.5 ± 0.2 °C at 10 cm depth) to +6 °C above ambient. Based on locals with long memories, relatively stable warming induced by geothermal hot spring activity has been present for at least 100 years while likely beyond 1000 years according to the historical records (Li and Wang, 1994). Soil radiocarbon Δ ^{14}C analysis for the surface sample (15 cm depth, <0.5 m away from geothermal hot springs) indicated that soil carbon has an age of 1250 years.

In this study, 6 transects in different directions were set along 6 replicated soil temperature gradients, and 4 field plots (ambient temperature, +2 °C, +4 °C and +6 °C warmed plots) were set in each soil temperature gradient within <25 m away from geothermal hot springs (Supplementary Fig. 1c). Therefore, these warmed field plots in these temperature gradients could be considered to represent SOC at the potential climax after a minimum of 1000 years of sustained warming with each gradient as a replicate block. Among all replicate blocks (n = 6), ambient temperature plots were similar in plant community composition, microbial biomass carbon, soil pH, moisture, ammonium, nitrate, total phosphorus, soil organic carbon and total nitrogen. We collected 24 soil samples in August 2020 and 2021, respectively. Specifically, each soil sample (0–15 cm depth) was taken from each ambient temperature plot or each warmed gradients plot. For each plot, three soil cores (2.5 cm diameter × 15 cm depth) were collected by a soil sampler tube and composited into one sample. Thus, a total of 48 soil samples were obtained from all ambient temperature and warmed plots.

2.2. Field measurements and ecosystem carbon fluxes

Soil temperature and moisture at the depth of 10 cm were measured *in situ* in each ambient temperature or warmed plot by using a portable soil temperature and moisture meter. Ecosystem carbon fluxes were measured *in situ* in each plot during the growing season in August 2023, including net ecosystem CO_2 exchange (NEE), ecosystem respiration (ER) and gross primary productivity (GPP). Specifically, a portable photosynthesis system (TARGAS-1, PP Systems, Amesbury, MA, USA) was used to determine NEE with a transparent chamber (30 cm × 30 cm × 30 cm), which covered all of the vegetation on the surface. Subsequently, ER was measured with the same method except that the transparent chamber was covered as a dark chamber with light shading material. All of these measurements were performed once or twice for each plot between 10:00 and 15:00 (local time). GPP was estimated as the difference between NEE and ER.

2.3. Bulk soil analysis

All soil samples were sieved with a 2-mm mesh to separate soil from plant roots and stones immediately after transportation to the laboratory at 4 °C. Roots with >1 cm length passed through the sieve were also removed from the soils with forceps. To determine SOC concentration, 1-g sieved soil was ground in ball mill for 24 h to about 100 mesh and analyzed by an Analytik Jena Multi N/C 3100 TOC analyzer. Microbial biomass carbon (MBC) was measured from all field fresh soil samples by using the chloroform fumigation extraction method (Soong et al., 2021). Briefly, one 10-g subsample was extracted by shaking in the 0.05 M K_2SO_4 solution for 1 h and then filtering with a Whatman #1, ash-free filter. The other 10-g subsample was fumigated with chloroform under vacuum for 3 days and then extracted in the above way. The extracts were analyzed for total organic carbon by an Analytik Jena Multi N/C 3100 TOC analyzer. MBC was calculated as the difference between the chloroform-fumigated and nonfumigated concentrations (Soong et al., 2021). To determine $\delta^{13}C$ (‰) in SOC, 2-g sieved soil was ground with stainless steel balls on a roller mill for 24 h and fully reacted with 0.5 M HCl until soil inorganic carbon being completely removed. Then, the soil samples were ultrasonically treated and freez-dried to constant weight. Finally, the $\delta^{13}C$ (‰) in SOC was analyzed by a Flash Combustion-Cavity Ring-Down Spectroscopy (CM-CRDS) Analyzer for all soil samples. Radiocarbon analysis was performed to estimate soil carbon age for one surface sample (15 cm depth, <0.5 m away from geothermal hot springs) by using 1-g dried soil in Xi 'an Accelerated Mass Spectrometry Center. Abundance of ^{14}C was measured using an IonPlus 200 keV MICADAS accelerator mass spectrometer (Cheng et al., 2013).

In addition to these soil carbon measurements, more soil chemical factors were determined in this study. Soil total nitrogen (TN) concentration was measured by using a Haineng K9840 Automatic Kjeldahl Azotometer (Liu et al., 2019). To measure soil ammonium and nitrate concentrations, 2-g field-moist sieved soil was suspended in a 2 M KCl solution and then analyzed using a Netherlands SKALAR San++ flow analyzer. Total phosphorus in soils was determined spectrophotometrically after digestion by HNO_3 and $HClO_4$ acid at 2000 °C with a subsample of 2-g field-moist sieved soil. Soil pH was measured using a pH meter with a calibrated combined glass electrode at a soil-to-water mass ratio of 1:2.5.

2.4. Soil organic carbon fractionation

To evaluate the responses of different SOC fractions to different warming levels, SOC in all soil samples was further separated into particulate organic carbon (POC, light fraction) and mineral-associated organic carbon (MAOC, heavy fraction), following a modified density fractionation technique (Liu et al., 2009; Rodriguez et al., 2014). Briefly, 5 g of each sieved (<2 mm) soil sample was weighed in a 50 mL centrifuge tube, and 60 mL of 1.8 g cm^{-3} NaI solution was added in the centrifuge tube. Then, all samples were shaken at 300 rpm for 2 h after dispersion by ultrasonication at 300 W and 40 KHz (SB25-12DTDN, Ningbo, China), and centrifuged at 3000 g for 15 min. After centrifuging, all samples were allowed to stand for 24 h, and then the supernatant (light fraction) was collected by pipetting. The procedure was repeated three times for each sample to ensure complete recovery of the light fraction. The sediment (heavy fraction) was collected in a new centrifuge tube. Subsequently, both the light fraction and the heavy fraction were washed by deionized water, over-dried at 60 °C to a constant weight, and then finely ground with stainless steel balls. Finally, SOC contents in the light and heavy fractions were determined using an Analytik Jena Multi N/C 3100 TOC analyzer.

2.5. Soil microbial carbon metabolic activity

To determine soil microbial metabolic activity under different warming levels, all 24 soil samples collected in 2021 were used to perform a short-term incubation experiment in the laboratory. Specifically, 5 treatments were set for each sample as follows: soil without any carbon substrates, soil with 8 mg glucose, soil with 8 mg cellulose, soil with 8 mg starch, and soil with 8 mg lignin. Thus, we filled each of 5 brown incubation flasks with 8 g soil and corresponding carbon substrate for each sample. After soil mixed fully with carbon substrates, the brown incubation flasks were sealed with rubber stoppers and incubated at room temperature for 30 days. Gas samples were collected from the headspace of the flasks, following ventilation and resealing for 1 h, in 1, 3, 5, 7, 10, 14, 20 and 30 days after addition of carbon substrates (Supplementary Figs. 2a–e). The concentration of CO_2 was measured with a GXH-3010E1 infrared CO_2 analyzer. We calculated mass-specific microbial respiration (μmol CO_2 gC_{mic}^{-1} h^{-1}) by multiplying CO_2 concentrations by bottles volume, then divided by the product of MBC, soil weight and time (Walker et al., 2018).

2.6. Microbial community analysis

Soil total DNA was extracted from 1-g soil and purified with a DNeasy PowerSoil Pro kit (Qiagen, Valencia, CA) according to the manufacturer's protocol. DNA quality was evaluated by a NanoDrop ND-1000 Spectrophotometer (NaoDrop Technologies, Wilmington, USA) on the basis of 260/280 nm and 260/230 nm absorbance ratios. All samples had 260/230 ratios >1.7 and 260/280 ratios >1.8. All DNA samples were stored at −80 °C until sequencing analysis.

Soil microbial community structures were analyzed using amplicon-based sequencing of 16 S ribosomal RNA genes for bacteria and archaea, and internal transcribed spacers (ITSs) for fungi. PCR amplification, library preparation and sequencing were performed in Magigene Biotechnology (Guangzhou, China). Specifically, the V4–V5 hypervariable region of bacterial and archaeal 16 S rRNA genes was amplified from 10 ng of DNA template with the universal primer set 515 forward (5′- GTGYCAGCMGCCGCGGTAA-3′) and 926 reverse (5′- CCGYCAATTYMTTTRAGTTT-3′) (Parada et al., 2016). The universal primer set ITS 5 forward (5′-GGAAGTAAAAGTCGTAACAAGG-3′) and ITS1 reverse (5′-GCTGCGTTCTTCATCGATGC-3′) was used to amplify fungal ITS sequence between 5.8 S and 28 S rRNA genes (Gu et al., 2017). A two-step PCR amplification method was used for library preparation to improve sequence representation and quantification (Wu et al., 2015; Guo et al., 2018; Yuan et al., 2021). First, 10 ng DNA from each sample was PCR-amplified for 10 cycles in triplicate in a 25 μl reaction volume with the primer sets for 16 S rRNA genes or ITS. The obtained triplicate PCR products were pooled, purified and eluted in 30 μl deionized water. In the second PCR amplification, 15 μl of the PCR products obtained from the first PCR amplification were PCR-amplified as template with primers containing sample-specific barcodes for 25 cycles. Subsequently, all PCR products were cleaned up and quantified by PicroGreen using a FLUOstar Optima fluorescence plant reader (BMG Labtech). PCR products from different samples were pooled at equal molality, and

sample libraries for sequencing were prepared according to the Illumina Nova Reagent Kit Preparation Guide. Finally, the mixed libraries were sequenced on Illumina Nova 6000 platform using 2 × 250 paired-end sequencing kit.

The raw reads of 16 S rRNA gene and ITS sequences were processed using an in-house pipeline. Briefly, the paired-end sequences were merged using FLASH (Magoč and Salzberg, 2011) after the primer sequences trimmed. Any merged sequences containing ambiguous bases or with a length of <330 bp for 16 S rRNA genes and <220 bp for ITS sequences were further removed. Subsequently, the high-quality 16 S rRNA gene or ITS sequences were used to generate zero-radius operational taxonomic units (zOTUs) by UNOISE3 (Edgar, 2018). To normalize samples to the same sequencing depth, 34,522 sequences for the 16 S rRNA gene and 46,778 sequences for the ITS were randomly selected for each sample. The representative 16 S rRNA gene sequences were taxonomically annotated by USEARCH 11 with Silva 132 Database (Glöckner et al., 2017) at a confidence cutoff of 50%, and chloroplast and mitochondria were further removed from the bacterial profiles. Taxonomic classification of ITS representative sequences were performed by taxonomically annotated with USEARCH 11 with UNITE Database (Version of 18.11.2018) (Nilsson et al., 2019) at a confidence cutoff of 50%.

2.7. Statistical analyses

Soil carbon/nitrogen pools and microbial physiology were analyzed using standardized linear mixed effects models to assess the effects of warming after accounting for the effects of the other key environmental factors (i.e., soil moisture and pH). The R packages lme4 and lmerTest were used to implement linear mixed effect models (Bates et al., 2015) with transect (that is, block) as a random intercept term. Since all ambient temperature and warmed plots had repeated measurements of SOC, total nitrogen (TN), $\delta^{13}C$, POC and MAOC in 2020 and 2021, sampling time (year) was also considered as a fixed effect in linear mixed effects models (y ~ warming level × moisture × pH + year + (1|block)). Effect sizes of warming or the other environmental factors were represented by the regression coefficients (β values) in linear mixed effects models. We also tested alternative models for SOC in which the effects of warming and sampling year were only considered as fixed effects (y ~ warming level × year + (1|block)). In addition, the effects of warming on SOC in each year were tested singly by linear mixed effects models (y ~ warming level+ (1|block)). All of these models indicated that there were significant warming effects on SOC concentration. Since the measurements of mass-specific microbial respiration were only performed for samples obtained in 2021, the following linear mixed effects models (y ~ warming level+ (1|block)) were used to test warming effects on mass-specific microbial respiration without or with carbon substrates. Due to the measurements of GPP, ER and NEE only in 2023, the following linear mixed effects models (y ~ warming level+ (1|block) or y ~ warming level × moisture × pH + (1|block)) were used to test warming effects on these ecosystem carbon fluxes. Paired *t*-test was performed to examine the significance of difference between the ambient temperature controls and different warming levels. The relationships of SOC concentration with different soil carbon pools (i.e., POC, MAOC and $\delta^{13}C$) were examined using Pearson correlation.

All statistical analyses for soil microbial communities were carried out using R software 3.1.1 with the package vegan (Oksanen et al., 2013) unless otherwise indicated. The effects of warming and the other key environmental factors (i.e., soil moisture and pH) on bacterial and fungal community structures was tested by the permutational multivariate analysis of variance (Adonis) based on Bray-Curtis dissimilarity matrices (Kruskal, 1964) considering the blocked design and repeated measurements. Principal coordinate analysis (PCoA) was further used to visualize the differences of bacterial and fungal community structure under ambient temperature control and different warming levels in a two-dimensional ordination space. Linear mixed effects models were used to test the warming effects on the relative abundance of bacterial and/or fungal phyla. And the top 10 abundant bacterial or fungal phyla were represented to show the shifts of phylum abundance in different warming levels. Redundancy analysis (RDA) was performed to assess the linkage between microbial communities and environmental factors. For individual environmental variable, soil carbon pool or microbial respiration, we performed Mantel tests to examine their correlations with microbial community structure (999 permutations).

3. Results and discussion

3.1. Soil organic carbon under warming

SOC concentrations were measured in all ambient temperature and warmed plots in this natural warming experiment of alpine grassland. Standardized linear mixed effects models indicated that warming significantly affected SOC concentration in both 2020 and 2021 ($\beta = -0.726$~-0.464, $P < 0.001$; Supplementary Table 1). Significant warming effects were still observed when combining the two years of data together after accounting for the effects of soil moisture, pH (7.76–9.81) and year ($\beta = -0.687$, $P < 0.001$; Fig. 1a and Supplementary Table 2). The similar effects of warming were observed on soil total nitrogen ($\beta = -0.687$, $P < 0.001$, Supplementary Table 2). Intriguingly, different warming levels led to completely different changes of SOC concentration (Fig. 1a). Specifically, there were no significant differences of SOC concentration between ambient temperature and +2 °C warmed field plots potentially after more than one thousand years of *in situ* warming, which is consistent with most observations under low-level warming conditions (Ding et al., 2017; Chen et al., 2022b). In contrast, the +4 °C warmed plots had significantly lost 6.78 + 1.92 g C kg^{-1} soil compared to the ambient temperature control plots, a deficit of 21.4 ± 6.0% in SOC stored in the top 15 cm (Fig. 1a). More SOC loss was observed in the +6 °C warmed plots, which is equal to 30.6 ± 5.2% SOC stored in the top 15 cm (Fig. 1a). Therefore, different warming levels had divergent effects on SOC, resulting in significant SOC losses of the alpine grassland under high level warming but not under low level warming.

3.2. Shifts of ecosystem carbon fluxes under warming

SOC is predominantly derived from the photosynthetic activities of surface vegetation (Henneron et al., 2020). Therefore, long-term warming may change SOC through influencing plant-mediated carbon fluxes. Interestingly, compared to the ambient plots in this site, both GPP and ER were significantly ($P < 0.001$, Fig. 1b–c) increased by warming, especially in the high-level warmed plots. Such changes led to significant increases of NEE in the warmed plots (Fig. 1d). Even when considering the influence of moisture and pH in the linear mixed effects models, warming still significantly enhanced the rates of ER ($P = 0.012$, Supplementary Table 3), GPP ($P = 0.006$, Supplementary Table 3), and NEE ($P = 0.027$, Supplementary Table 3) in this alpine grassland ecosystem. These results were consistent with previous studies that warming could alleviate temperature limitations on plant growth, thus promoting plant growth and productivity in most area of the Qinghai-Tibet Plateau (Chen et al., 2022a). Warming-enhanced NEE could promote more soil carbon input as plant litter, root biomass or exudates in this alpine grassland ecosystem (Guo et al., 2020). Logically, such changes could lead to SOC increases, not decreases under long-term warming. Therefore, plant-mediated carbon fluxes appear to less likely explain significant SOC losses under high level warming.

3.3. Microbial decomposition of soil organic carbon

Warming-induced SOC losses in this alpine grassland could be due to the changes in SOC chemical and physical composition. Since soil microbes preferentially respire ^{12}C resulting in enriched ^{13}C in SOC during decomposition (Natelhoffer and Fry, 1988; Soong et al., 2021), the $\delta^{13}C$

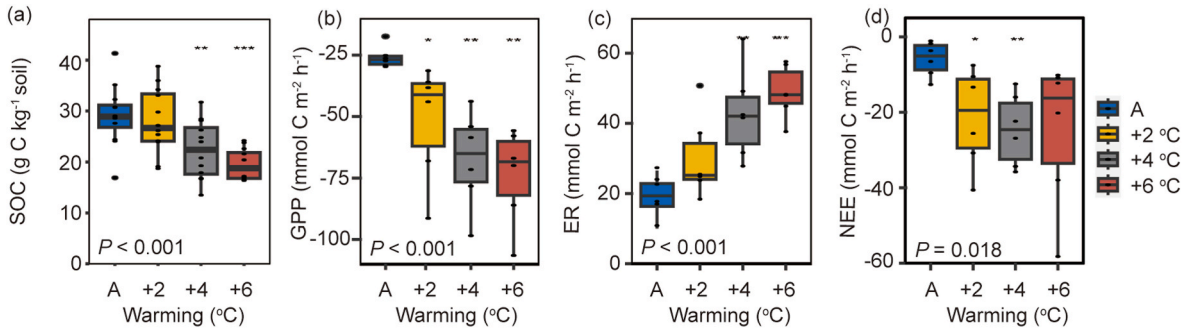

Fig. 1. Changes of SOC and ecosystem carbon fluxes under different warming levels. **(a)** Soil organic carbon (SOC) concentration across 2020 and 2021. **(b)** Gross primary productivity (GPP) in 2023. **(c)** Ecological respiration (ER) rates in 2023. **(d)** Net ecosystem exchange (NEE) in 2023. Six replicate samples were investigated in each year ($n = 6$). Ecosystem carbon fluxes were estimated on the basis of the carbon amount from CO_2 emissions. Positive values indicate carbon source, and negative values represent carbon sink. Significance of warming effects were tested by the linear mixed-effects models (Supplementary Tables 2 and 3), and P values are shown in each plot. Significant differences between different warming levels and ambient temperature (A) are labeled, and non-significant changes are not labeled. P values of the t-test are labeled by *** when $P < 0.001$, ** when $P < 0.01$, and * when $P < 0.05$.

of SOC can characterize the degree of SOC degradation (Natelhoffer and Fry, 1988; Soong et al., 2021). The standardized linear mixed effects model showed that warming had significantly positive effects on $\delta^{13}C$ ($\beta = 0.476$, $P = 0.019$; Supplementary Table 2), that is, $\delta^{13}C$ increased with warming levels compared to the ambient control plots (Fig. 2a). Meanwhile, the $\delta^{13}C$ exhibited a significantly negative correlation with SOC concentration ($R^2 = 0.554$, $P < 0.001$; Fig. 2b). Therefore, the enrichment of ^{13}C in higher level warmed soils indicates more degraded SOC than the ambient control soils (Dijkstra et al., 2006). However, such more degraded SOC didn't necessarily resulted in more microbial biomass in the warmed soils. In fact, soil microbial biomass carbon (MBC) was significantly decreased by warming especially higher levels of warming ($\beta = -0.335$, $P < 0.001$; Fig. 2c and Supplementary Table 2), suggesting less microbial biomass obtained with more degraded SOC under warming. This was confirmed by a one-month incubation experiment without addition of any carbon substrates, in which soil

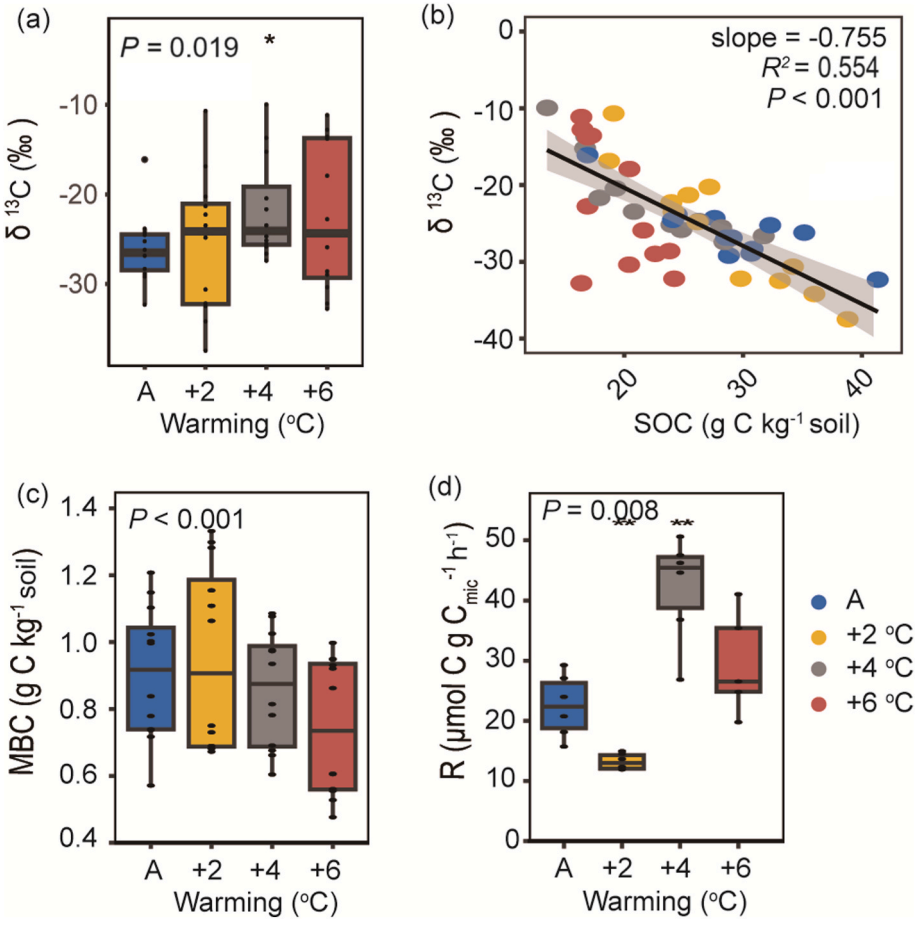

Fig. 2. Soil $\delta^{13}C$, microbial biomass carbon and respiration under different warming levels. **(a)** $\delta^{13}C$ (‰) across 2020 and 2021. **(b)** SOC exhibited significantly negative correlation with $\delta^{13}C$ across 2020 and 2021. The slope, pearson correlation coefficients (R^2) and P values from linear regressions are shown in the plot. **(c)** Microbial biomass carbon (MBC) across 2020 and 2021. **(d)** Mass-specific microbial carbon (R) in 2021. Samples from ambient temperature (A) and different warming levels (+2 °C to +6 °C) are labeled by different colors. P values of the t-test are labeled by *** when $P < 0.001$, ** when $P < 0.01$, and * when $P < 0.05$.

mass-specific microbial respiration (i.e., microbial respiration per unit of biomass) significantly increased by 77.9%–97.9% under +4~+6 °C warming levels, but decreased by 38.8% under +2 °C warming level (β = 0.524, $P = 0.008$; Fig. 2d and Supplementary Table 4). Consistently, soil incubation experiments with additions of glucose, starch, cellulose or lignin further documented that more substrate carbon in warmed soils was allocated for microbial respiration rather than growth (Supplementary Figs. 3a–d and Supplementary Table 4), thus potentially resulting in the decline of microbial carbon use efficiency. Taken together, these results indicated that high level warming promoted microbial SOC degradation and respiration, potentially accompanied by a decline of microbial carbon use efficiency, thus leading to the SOC loss in alpine grassland.

3.4. Particulate organic carbon (POC) and mineral-associated organic carbon (MAOC)

SOC is a heterogeneous mixture, spanning partially decomposed plant particulates to microbial residues, which are physically protected from microbial decomposition via adsorption to reactive mineral surfaces or by soil aggregates to varying degrees (Lehmann and Kleber, 2015). Such mechanisms of physical stabilization are extremely important for maintaining the stability of SOC (Lehmann and Kleber, 2015). However, it is largely unknown how different warming levels affect differing physical compositions of SOC. To address this issue, we fractionated the SOC of alpine grassland into particulate organic carbon (POC), which mostly consists of plant-derived organic particulates and is relatively accessible to microbial decomposition; and mineral-associated organic carbon (MAOC), which is comprised of more microbially-catabolized organic matter that is protected by association with reactive mineral surfaces or within microaggregates (Soong et al., 2021). Low litter input to the soil due to low air temperature in this alpine region lead to relatively small POM pools but large MAOC pools (Guo et al., 2022a). Previous short-term studies indicated that POC presents much shorter turnover times and is sensitive to warming, while MAOC is older organic carbon and not easily affected by warming (Guo et al., 2022b). However, we found that MAOC rather than POC was significantly (β = −0.461, $P = 0.022$) affected by long-term *in situ* warming as indicated by linear mixed effects models (Fig. 3a–b and Supplementary Table 5). The decline of MAOC became more obvious with warming levels compared to the ambient control plots. Specifically, MAOC had no significant change in +2 °C warmed plots, but decreased by 10.0 ± 6.8% and 20.4 ± 7.1% in +4 °C and +6 °C warmed plots separately (Fig. 3b). Furthermore, significantly positive correlation was observed between MAOC and SOC ($R^2 = 0.913$, $P < 0.001$; Fig. 3d), which is much more significant than the correlation between POC and SOC ($R^2 = 0.258$, $P < 0.001$; Fig. 3c). Therefore, the losses of alpine grassland SOC caused by high-level warming were mainly due to the decline of MAOC rather than POC.

3.5. Linkages between microbial community and soil carbon cycling

The magnitude of SOC could substantially depend upon microbial involvement, since SOC dynamics are ultimately the consequence of microbial activity (Liang et al., 2017). Therefore, microbial mechanisms responsible for warming-induced soil carbon loss are the subject of intense scientific debate in recent decades (Liang et al., 2017; Walker et al., 2018). While the SOC pools at the potential climax definitely

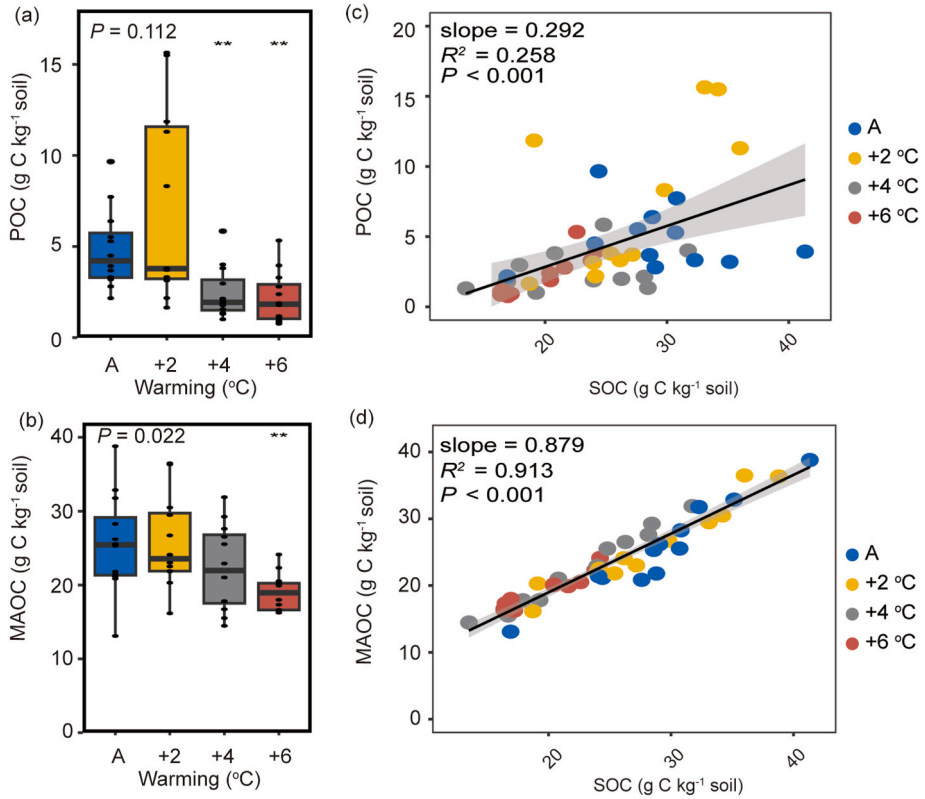

Fig. 3. Soil organic carbon fractions under different warming levels. **(a)** Particulate organic carbon (POC) across 2020 and 2021. **(b)** Mineral-associated organic carbon (MAOC) across 2020 and 2021. Six replicate samples were investigated in each year ($n = 6$). Significance of warming effects were tested by the linear mixed-effects models (Supplementary Table 5), and *P* values are shown in each plot. Significant differences between different warming levels and ambient temperature (A) are labeled, and non-significant changes are not labeled. *P* values of the *t*-test are labeled by ** when $P < 0.01$, and * when $P < 0.05$. **(c)** Correlation between POC and soil organic carbon (SOC). **(d)** Correlation between MAOC and SOC. The slope, pearson correlation coefficients (R^2) and *P* values from linear regressions are shown in each plots.

could not be observed in most warming manipulation experiments, as the durations of these experiments are far shorter than soil carbon turnover times, various associated microbial mechanisms have been documented including depletion of microbially accessible carbon pools, reductions in microbial biomass, changes in microbial carbon use efficiency, and shifts in microbial community structure (Melillo et al., 2017; Walker et al., 2018; Guo et al., 2020). Logically, these microbial mechanisms should be still responsible for soil carbon dynamics when the final and stable stage of SOC pools has been reached after a long enough period of warming. Our analysis for these geothermal warmed soils in alpine grassland confirmed that there were significant decline of soil MAOC pools, decrease of microbial biomass, and decline of microbial carbon use efficiency along SOC losses under high-level warming. To further identify the importance of microbial community structures for the warming-induced SOC losses, Amplicon-based sequencing of 16 S ribosomal RNA (16 S rRNA) genes and internal transcribed spacers (ITSs) were used to analyze community structures of bacteria and fungi.

Warming-induced changes of microbial community structures had been observed in many previous short-term studies (Zhou et al., 2012; Guo et al., 2020). In this study, long-term *in situ* warming markedly shifted bacterial and fungal community structures compared to the ambient controls in both 2020 and 2021, as indicated by principal coordinates analysis (PCoA) based on Bray-Curtis dissimilarity matrices (Fig. 4a–b). The shifts of bacterial and fungal communities under high-level warming were obviously larger than those under low-level warming. Permutational multivariate statistical tests revealed that bacterial and fungal community structures were significantly ($P < 0.001$) altered by warming (Supplementary Table 6). Furthermore, warming significantly altered the relative abundances of many bacterial and fungal phyla (Fig. 4c–d and Supplementary Table 7). For instance, the relative abundance of *Actinobacteria* and *Ascomycota* were significantly decreased with warming levels, while *Chloroflexi* and *Basidiomycota* were significantly increased with warming levels. Furthermore, a significantly positive correlation ($\beta = 0.303$, $P = 0.036$; Supplementary Table 8) was observed between SOC and *Ascomycota*, a typically copiotrophic phylum (Yao et al., 2017), suggesting a potential indicator for soil carbon change under warming. Altogether, these results indicated that high level warming could more significantly shift soil microbial community composition and structure than low level warming.

The shifts of microbial communities by warming seem to play significant roles in the losses of alpine grassland SOC. First, both redundancy analysis (RDA) and Mantel test showed that bacterial and fungal community structures were tightly linked to several key environmental factors, including soil temperature, moisture and pH (Fig. 4e and Supplementary Fig. 4). Among all environmental factors, soil temperature exhibited the largest impacts ($r = 0.441$–0.474, $P < 0.001$) on both bacterial and fungal communities (Fig. 4e and Supplementary Table 9). Expectedly, significant correlations of microbial communities were observed with SOC and its components MAOC and POC in Mantel test (Fig. 4e). Soil bacterial and fungal communities also exhibited significant correlations with related parameters (i.e., MBC and $\delta^{13}C$) of microbial carbon cycling (Fig. 4e). Furthermore, both bacterial and fungal communities also showed strong ($r = 0.500$–0.661, $P < 0.001$) correlations with soil mass-specific microbial respiration (Supplementary

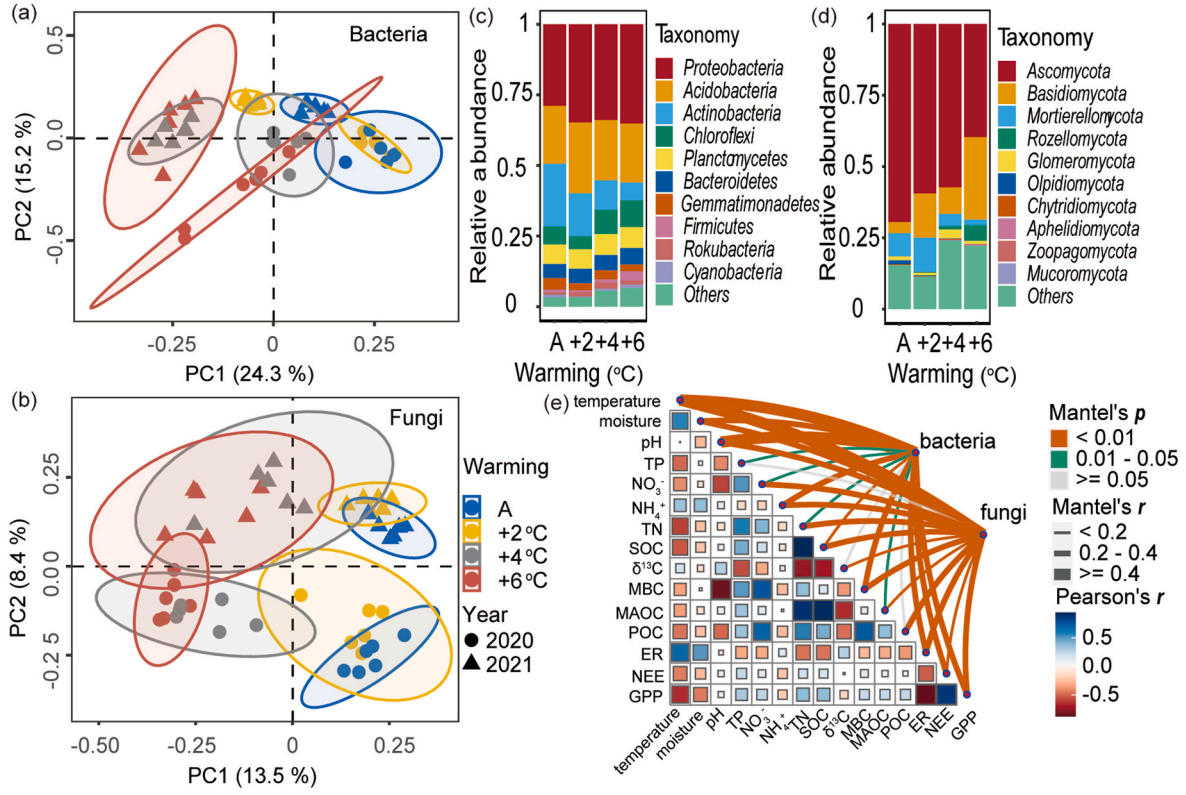

Fig. 4. Microbial mechanisms responsible for SOC changes in response to different warming levels. (a) Principal coordinates analysis (PCoA) of soil bacterial community structures based on Bray-Curtis dissimilarity matrices. **(b)** PCoA of soil fungal community structures based on Bray-Curtis dissimilarity matrices. **(c)** Relative abundance of bacterial phyla under different warming levels or ambient temperature (A) across 2020 and 2021. **(d)** Relative abundance of fungal phyla under different warming levels or ambient temperature (A) across 2020 and 2021. **(e)** Pairwise comparisons of soil carbon pools and environmental factors with correlations of bacterial and fungal community structures. Microbial community structures were related to each soil carbon pools or environmental factor by Mantel tests. Edge width represents the Mantel's *r* statistic for the corresponding correlations, and edge color denotes the statistical significance. The orange line indicates a significant correlation ($P < 0.01$) between environmental factors and bacterial or fungal communities by Mantel test. The green line indicates a significant correlation ($0.01 < P < 0.05$) between environmental factors and bacterial or fungal communities by Mantel test. The abbreviations are the same as Figs. 1–3. TP: total phosphorus; TN: total nitrogen.

Table 9). These results indicated that warming-induced shifts in community structures of soil bacteria and fungi were strongly correlated with SOC and associated carbon cycling processes, suggesting microbial significant roles in controlling the losses of alpine grassland SOC.

4. Conclusion and implication

Quantifying warming-induced changes of SOC is urgently needed to improve modeling projections for future climate warming scenarios (Crowther et al., 2016). However, the direct field measurements of the responses of SOC to warming are scarce, especially when an ecosystem reaches to the potential climax community after a long enough period of warming. Most soil carbon-climate models must rely on the short-term temperature responses of soil respiration to infer long-term SOC changes (Bradford et al., 2016; Crowther et al., 2016), which is bound to lead to large uncertainties in model projections. Such uncertainties could be even worse for projecting the changes of huge SOC stocks in cold regions, since soil carbon turnover times in cold regions are much longer than the rest of the world (Wang et al., 2018). Meanwhile, these cold regions are expected to be threatened by more serious climate warming in this century (Chen et al., 2013; Cohen et al., 2014; Jia et al., 2017). Therefore, the destabilization of SOC caused by climate warming in cold regions attracts a lot of attentions (Ding et al., 2017; Walker et al., 2018; Wu et al., 2021).

In this study, we showed that SOC was significantly lost under high-level warming (+4~+6 °C), but remained unchanged under low-level of warming (+2 °C). This is evidenced using direct filed measurements from geothermal warming gradients when the alpine grassland ecosystem potentially close to the climax community, which could not be concluded based on short-term warming experiments or only based on ecosystem carbon fluxes alone. If this phenomenon holds over large spatial scales in cold regions, the losses of SOC induced by high-level warming would greatly amplify global climate warming by releasing huge amounts of carbon to the atmosphere, while low-level warming would not trigger this catastrophe. Our study also revealed that the losses of SOC induced by high-level warming were primarily from MAOC rather than unprotected plant-derived POC. Given that MAOC has much longer turnover times than POC(Guo et al., 2022b), such SOC losses are likely to be permanent rather than recoverable in a short time. In addition, our study revealed that the shifts of soil microbial communities and associated decline of microbial carbon use efficiency were responsible for SOC changes of alpine grassland under different warming levels. Ultimately, our study suggested that models must account for these heterogeneous responses of SOC to different warming levels for projecting future climate scenarios.

CRediT authorship contribution statement

Zhengxiong Liang: Writing – original draft. **Xue Guo:** Writing – review & editing, Writing – original draft, Methodology, Formal analysis, Data curation. **Suo Liu:** Methodology. **Yifan Su:** Data curation. **Yufei Zeng:** Methodology. **Changyi Xie:** Formal analysis. **Qun Gao:** Supervision. **Jiesi Lei:** Data curation. **Baochan Li:** Data curation. **Mei Wang:** Project administration. **Tianjiao Dai:** Investigation. **Liyuan Ma:** Resources. **Fenliang Fan:** Visualization, Supervision, Resources. **Yunfeng Yang:** Funding acquisition. **Xuehua Liu:** Supervision. **Jizhong Zhou:** Supervision.

Declaration of competing interest

We have no known competing financial interests or personal relationship that could have appeared to influence the work reported in this paper.

Data availability

Data will be made available on request.

Acknowledgments

The authors are grateful to the numerous laboratory members for their help in maintaining the experimental site. This research is supported by the National Natural Science Foundation of China (42277213,41825016 and 41907209), the Second Tibetan Plateau Scientific Expedition and Research (STEP) program (2019QZKK0503), the Hundred Talents Program of the Chinese Academy of Sciences (CAS) and the CAS Youth Interdisciplinary Team.

Appendix A. Supplementary data

Supplementary data to this article can be found online at https://doi.org/10.1016/j.soilbio.2024.109395.

References

Bates, D., Mächler, M., Bolker, B., Walker, S., 2015. Fitting linear mixed-effects models using lme4. Journal of Statistical Software 67, 1–48.
Bradford, M.A., Wieder, W.R., Bonan, G.B., Fierer, N., Raymond, P.A., Crowther, T.W., 2016. Managing uncertainty in soil carbon feedbacks to climate change. Nature Climate Change 6, 751–758.
Chen, H., Ju, P., Zhu, Q., Xu, X., Wu, N., Gao, Y., Feng, X., Tian, J., Niu, S., Zhang, Y., Peng, C., Wang, Y., 2022a. Carbon and nitrogen cycling on the Qinghai–Tibetan plateau. Nature Reviews Earth & Environment 3, 701–716.
Chen, H., Zhu, Q., Peng, C., Wu, N., Wang, Y., Fang, X., Gao, Y., Zhu, D., Yang, G., Tian, J., Kang, X., Piao, S., Ouyang, H., Xiang, W., Luo, Z., Jiang, H., Song, X., Zhang, Y., Yu, G., Zhao, X., Gong, P., Yao, T., Wu, J., 2013. The impacts of climate change and human activities on biogeochemical cycles on the Qinghai-Tibetan Plateau. Global Change Biology 19, 2940–2955.
Chen, Y., Han, M., Yuan, X., Hou, Y., Qin, W., Zhou, H., Zhao, X., Klein, J.A., Zhu, B., 2022b. Warming has a minor effect on surface soil organic carbon in alpine meadow ecosystems on the Qinghai–Tibetan Plateau. Global Change Biology 28, 1618–1629.
Chen, Y., Han, M., Yuan, X., Zhou, H., Zhao, X., Schimel, J.P., Zhu, B., 2023. Long-term warming reduces surface soil organic carbon by reducing mineral-associated carbon rather than "free" particulate carbon. Soil Biology and Biochemistry 177.
Cheng, P., Zhou, W., Wang, H., Lu, X., Du, H., 2013. 14C dating of soil organic carbon (SOC) in loess-paleosol using sequential pyrolysis and accelerator mass spectrometry (AMS). Radiocarbon 55, 563–570.
Cohen, J., Screen, J.A., Furtado, J.C., Barlow, M., Whittleston, D., Coumou, D., Francis, J., Dethloff, K., Entekhabi, D., Overland, J., Jones, J., 2014. Recent Arctic amplification and extreme mid-latitude weather. Nature Geoscience 7, 627–637.
Collins, C.G., Elmendorf, S.C., Hollister, R.D., Henry, G.H.R., Clark, K., Bjorkman, A.D., Myers-Smith, I.H., Prevéy, J.S., Ashton, I.W., Assmann, J.J., Alatalo, J.M., Carbognani, M., Chisholm, C., Cooper, E.J., Forrester, C., Jónsdóttir, I.S., Klanderud, K., Kopp, C.W., Livensperger, C., Mauritz, M., May, J.L., Molau, U., Oberbauer, S.F., Ogburn, E., Panchen, Z.A., Petraglia, A., Post, E., Rixen, C., Rodenhizer, H., Schuur, E.A.G., Semenchuk, P., Smith, J.G., Steltzer, H., Totland, Ø., Walker, M.D., Welker, J.M., Suding, K.N., 2021. Experimental warming differentially affects vegetative and reproductive phenology of tundra plants. Nature Communications 12, 3442.
Crowther, T.W., Todd-Brown, K.E.O., Rowe, C.W., Wieder, W.R., Carey, J.C., Machmuller, M.B., Snoek, B.L., Fang, S., Zhou, G., Allison, S.D., Blair, J.M., Bridgham, S.D., Burton, A.J., Carrillo, Y., Reich, P.B., Clark, J.S., Classen, A.T., Dijkstra, F.A., Elberling, B., Emmett, B.A., Estiarte, M., Frey, S.D., Guo, J., Harte, J., Jiang, L., Johnson, B.R., Kröel-Dulay, G., Larsen, K.S., Laudon, H., Lavallee, J.M., Luo, Y., Lupascu, M., Ma, L.N., Marhan, S., Michelsen, A., Mohan, J., Niu, S., Pendall, E., Peñuelas, J., Pfeifer-Meister, L., Poll, C., Reinsch, S., Reynolds, L.L., Schmidt, I.K., Sistla, S., Sokol, N.W., Templer, P.H., Treseder, K.K., Welker, J.M., Bradford, M.A., 2016. Quantifying global soil carbon losses in response to warming. Nature 540, 104–108.
de Vrese, P., Brovkin, V., 2021. Timescales of the permafrost carbon cycle and legacy effects of temperature overshoot scenarios. Nature Communications 12, 2688.
Dijkstra, P., Ishizu, A., Doucett, R., Hart, S.C., Schwartz, E., Menyailo, O.V., Hungate, B. A., 2006. 13C and 15N natural abundance of the soil microbial biomass. Soil Biology and Biochemistry 38, 3257–3266.
Ding, J., Chen, L., Ji, C., Hugelius, G., Li, Y., Liu, L., Qin, S., Zhang, B., Yang, G., Li, F., Fang, K., Chen, Y., Peng, Y., Zhao, X., He, H., Smith, P., Fang, J., Yang, Y., 2017. Decadal soil carbon accumulation across Tibetan permafrost regions. Nature Geoscience 10, 420–424.
Edgar, R.C., 2018. Updating the 97% identity threshold for 16S ribosomal RNA OTUs. Bioinformatics 34, 2371–2375.
Erb, K.-H., Fetzel, T., Plutzar, C., Kastner, T., Lauk, C., Mayer, A., Niedertscheider, M., Körner, C., Haberl, H., 2016. Biomass turnover time in terrestrial ecosystems halved by land use. Nature Geoscience 9, 674–678.

Fang, C., Li, F., Pei, J., Ren, J., Gong, Y., Yuan, Z., Ke, W., Zheng, Y., Bai, X., Ye, J.-S., 2018. Impacts of warming and nitrogen addition on soil autotrophic and heterotrophic respiration in a semi-arid environment. Agricultural and Forest Meteorology 248, 449–457.
Garcia-Palacios, P., Escolar, C., Dacal, M., Delgado-Baquerizo, M., Gozalo, B., Ochoa, V., Maestre, F.T., 2018. Pathways regulating decreased soil respiration with warming in a biocrust-dominated dryland. Global Change Biology 24, 4645–4656.
Glöckner, F.O., Yilmaz, P., Quast, C., Gerken, J., Beccati, A., Ciuprina, A., Bruns, G., Yarza, P., Peplies, J., Westram, R., Ludwig, W., 2017. 25 years of serving the community with ribosomal RNA gene reference databases and tools. Journal of Biotechnology 261, 169–176.
Gu, W., Lu, Y., Tan, Z., Xu, P., Xie, K., Li, X., Sun, L., 2017. Fungi diversity from different depths and times in chicken manure waste static aerobic composting. Bioresource Technology 239, 447–453.
Guo, M., Zhao, B., Wen, Y., Hu, J., Dou, A., Zhang, Z., Rui, J., Li, W., Wang, Q., Zhu, J., 2022a. Elevational pattern of soil organic carbon release in a Tibetan alpine grassland: consequence of quality but not quantity of initial soil organic carbon. Geoderma 428, 116148.
Guo, X., Feng, J., Shi, Z., Zhou, X., Yuan, M., Tao, X., Hale, L., Yuan, T., Wang, J., Qin, Y., Zhou, A., Fu, Y., Wu, L., He, Z., Van Nostrand, J.D., Ning, D., Liu, X., Luo, Y., Tiedje, J.M., Yang, Y., Zhou, J., 2018. Climate warming leads to divergent succession of grassland microbial communities. Nature Climate Change 8, 813–818.
Guo, X., Gao, Q., Yuan, M., Wang, G., Zhou, X., Feng, J., Shi, Z., Hale, L., Wu, L., Zhou, A., Tian, R., Liu, F., Wu, B., Chen, L., Jung, C.G., Niu, S., Li, D., Xu, X., Jiang, L., Escalas, A., Wu, L., He, Z., Van Nostrand, J.D., Ning, D., Liu, X., Yang, Y., Schuur, E.A.G., Konstantinidis, K.T., Cole, J.R., Penton, C.R., Luo, Y., Tiedje, J.M., Zhou, J., 2020. Gene-informed decomposition model predicts lower soil carbon loss due to persistent microbial adaptation to warming. Nature Communications 11, 4897.
Guo, X., Viscarra Rossel, R.A., Wang, G., Xiao, L., Wang, M., Zhang, S., Luo, Z., 2022b. Particulate and mineral-associated organic carbon turnover revealed by modelling their long-term dynamics. Soil Biology and Biochemistry 173, 108780.
Hararuk, O., Smith, M.J., Luo, Y., 2015. Microbial models with data-driven parameters predict stronger soil carbon responses to climate change. Global Change Biology 21, 2439–2453.
He, Y., Trumbore, S.E., Torn, M.S., Harden, J.W., Vaughn, L.J.S., Allison, S.D., Randerson, J.T., 2016. Radiocarbon constraints imply reduced carbon uptake by soils during the 21st century. Science 353, 1419–1424.
Heimann, M., Reichstein, M., 2008. Terrestrial ecosystem carbon dynamics and climate feedbacks. Nature 451, 289–292.
Henneron, L., Cros, C., Picon-Cochard, C., Rahimian, V., Fontaine, S., 2020. Plant economic strategies of grassland species control soil carbon dynamics through rhizodeposition. Journal of Ecology 108, 528–545.
Hugelius, G., Strauss, J., Zubrzycki, S., Harden, J.W., Schuur, E.A.G., Ping, C.L., Schirrmeister, L., Grosse, G., Michaelson, G.J., Koven, C.D., O'Donnell, J.A., Elberling, B., Mishra, U., Camill, P., Yu, Z., Palmtag, J., Kuhry, P., 2014. Estimated stocks of circumpolar permafrost carbon with quantified uncertainty ranges and identified data gaps. Biogeosciences 11, 6573–6593.
Intergovernmental Panel on Climate, C., 2014. Climate Change 2013 – the Physical Science Basis: Working Group I Contribution to the Fifth Assessment Report of the Intergovernmental Panel on Climate Change. Cambridge University Press, Cambridge.
Jia, J., Feng, X., He, J.-S., He, H., Lin, L., Liu, Z., 2017. Comparing microbial carbon sequestration and priming in the subsoil versus topsoil of a Qinghai-Tibetan alpine grassland. Soil Biology and Biochemistry 104, 141–151.
Kruskal, J.B., 1964. Nonmetric multidimensional scaling: a numerical method. Psychometrika 29, 115–129.
Lehmann, J., Kleber, M., 2015. The contentious nature of soil organic matter. Nature 528, 60–68.
Li, C., Peng, F., Xue, X., You, Q., Lai, C., Zhang, W., Cheng, Y., 2018. Productivity and quality of alpine grassland vary with soil water availability under experimental warming. Frontiers in Plant Science 9.
Li, Q., Wang, Y., 1994. Records of Haiyan County 海晏县志. Gansu Culture Publishing House, Lanzhou.
Liang, C., Schimel, J.P., Jastrow, J.D., 2017. The importance of anabolism in microbial control over soil carbon storage. Nature Microbiology 2, 17105.
Liu, L., King, J.S., Booker, F.L., Giardina, C.P., Lee Allen, H., Hu, S., 2009. Enhanced litter input rather than changes in litter chemistry drive soil carbon and nitrogen cycles under elevated CO2: a microcosm study. Global Change Biology 15, 441–453.
Liu, M., Sui, X., Hu, Y., Feng, F., 2019. Microbial community structure and the relationship with soil carbon and nitrogen in an original Korean pine forest of Changbai Mountain, China. BMC Microbiology 19.
Magoč, T., Salzberg, S.L., 2011. FLASH: fast length adjustment of short reads to improve genome assemblies. Bioinformatics 27, 2957–2963.
Melillo, J.M., Frey, S.D., DeAngelis, K.M., Werner, W.J., Bernard, M.J., Bowles, F.P., Pold, G., Knorr, M.A., Grandy, A.S., 2017. Long-term pattern and magnitude of soil carbon feedback to the climate system in a warming world. Science 358, 101–105.
Meng, C., Tian, D., Zeng, H., Li, Z., Chen, H.Y.H., Niu, S., 2020. Global meta-analysis on the responses of soil extracellular enzyme activities to warming. Sci Total Environ 705, 135992.
Natelhoffer, K.J., Fry, B., 1988. Controls on natural nitrogen-15 and carbon-13 abundances in forest soil organic matter. Soil Science Society of America Journal 52, 1633–1640.
Nilsson, R.H., Larsson, K.-H., Taylor, A.F.S., Bengtsson-Palme, J., Jeppesen, T.S., Schigel, D., Kennedy, P., Picard, K., Glöckner, F.O., Tedersoo, L., Saar, I., Kõljalg, U., Abarenkov, K., 2019. The UNITE database for molecular identification of fungi: handling dark taxa and parallel taxonomic classifications. Nucleic Acids Research 47, D259–D264.
O'Gorman, E.J., Benstead, J.P., Cross, W.F., Friberg, N., Hood, J.M., Johnson, P.W., Sigurdsson, B.D., Woodward, G., 2014. Climate change and geothermal ecosystems: natural laboratories, sentinel systems, and future refugia. Global Change Biology 20, 3291–3299.
O'Gorman, E.J., Zhao, L., Pichler, D.E., Adams, G., Friberg, N., Rall, Björn C., Seeney, A., Zhang, H., Reuman, D.C., Woodward, G., 2017. Unexpected changes in community size structure in a natural warming experiment. Nature Climate Change 7, 659–663.
Oksanen, J., Blanchet, F.G., Kindt, R., Legendre, P., Minchin, P., O'Hara, R.B., Simpson, G., Solymos, P., Stevens, M.H.H., Wagner, H., 2013. Vegan: Community Ecology Package. R Package Version. 2.0-10. CRAN.
Parada, A.E., Needham, D.M., Fuhrman, J.A., 2016. Every base matters: assessing small subunit rRNA primers for marine microbiomes with mock communities, time series and global field samples. Environmental Microbiology 18, 1403–1414.
Qi, Q., Haowei, Y., Zhang, Z., Nostrand, J.D.V., Wu, L., Guo, X., Feng, J., Wang, M., Yang, S., Zhao, J., Gao, Q., Zhang, Q., Zhao, M., Xie, C., Ma, Z., He, J.-S., Chu, H., Huang, Y., Zhou, J., Yang, Y., DeAngelis, K.M., Lovley, D.R., 2021. Microbial functional responses explain alpine soil carbon fluxes under future climate scenarios. mBio 12, e00761-00720.
Reich, P.B., Sendall, K.M., Stefanski, A., Rich, R.L., Hobbie, S.E., Montgomery, R.A., 2018. Effects of climate warming on photosynthesis in boreal tree species depend on soil moisture. Nature 562, 263–267.
Rodriguez, A., Lovett, G.M., Weathers, K.C., Arthur, M.A., Templer, P.H., Goodale, C.L., Christenson, L.M., 2014. Lability of C in temperate forest soils: assessing the role of nitrogen addition and tree species composition. Soil Biology and Biochemistry 77, 129–140.
Schmidt, M.W.I., Torn, M.S., Abiven, S., Dittmar, T., Guggenberger, G., Janssens, I.A., Kleber, M., Kögel-Knabner, I., Lehmann, J., Manning, D.A.C., Nannipieri, P., Rasse, D.P., Weiner, S., Trumbore, S.E., 2011. Persistence of soil organic matter as an ecosystem property. Nature 478, 49–56.
Sigurdsson, B.D., Leblans, N.I.W., Dauwe, S., Guðmundsdóttir, E., Gundersen, P., Gunnarsdóttir, G.E.G., Holmstrup, M., Ilieva-Makulec, K., Kätterer, T., Marteinsdóttir, B., Maljanen, M., Oddsdóttir, E.S., Ostonen, I., Peñuelas, J., Poeplau, C., Richter, A., Sigurðsson, P., Bodegom, P.M.v., Wallander, H., Weedon, J. T., Janssens, I.A., 2016. Geothermal ecosystems as natural climate change experiments: the ForHot research site in Iceland as a case study. Icelandic Agricultural Sciences 29, 53–71.
Soong, J.L., Castanha, C., Hicks Pries, C.E., Ofiti, N., Porras, R.C., Riley, W.J., Schmidt, M.W.I., Torn, M.S., 2021. Five years of whole-soil warming led to loss of subsoil carbon stocks and increased CO2 efflux. Science Advances 7, eabd1343.
Todd-Brown, K., Zheng, B., Crowther, T.W., 2018. Field-warmed soil carbon changes imply high 21st-century modeling uncertainty. Biogeosciences 15, 3659–3671.
van Gestel, N., Shi, Z., van Groenigen, K.J., Osenberg, C.W., Andresen, L.C., Dukes, J.S., Hovenden, M.J., Luo, Y., Michelsen, A., Pendall, E., Reich, P.B., Schuur, E.A.G., Hungate, B.A., 2018. Predicting soil carbon loss with warming. Nature 554, E4–E5.
Walker, T.W.N., Kaiser, C., Strasser, F., Herbold, C.W., Leblans, N.I.W., Woebken, D., Janssens, I.A., Sigurdsson, B.D., Richter, A., 2018. Microbial temperature sensitivity and biomass change explain soil carbon loss with warming. Nature Climate Change 8, 885–889.
Wang, J., Quan, Q., Chen, W., Tian, D., Ciais, P., Crowther, T.W., Mack, M.C., Poulter, B., Tian, H., Luo, Y., Wen, X., Yu, G., Niu, S., 2021. Increased CO2 emissions surpass reductions of non-CO2 emissions more under higher experimental warming in an alpine meadow. Science of The Total Environment 769, 144559.
Wang, J., Sun, J., Xia, J., He, N., Li, M., Niu, S., 2018. Soil and vegetation carbon turnover times from tropical to boreal forests. Functional Ecology 32, 71–82.
Wang, Q., Lv, W., Li, B., Zhou, Y., Jiang, L., Piao, S., Wang, Y., Zhang, L., Meng, F., Liu, P., Hong, H., Li, Y., Dorji, T., Luo, C., Zhang, Z., Ciais, P., Peñuelas, J., Kardol, P., Zhou, H., Wang, S., 2020. Annual ecosystem respiration is resistant to changes in freeze–thaw periods in semi-arid permafrost. Global Change Biology 26, 2630–2641.
Wu, D., Liu, D., Wang, T., Ding, J., He, Y., Ciais, P., Zhang, G., Piao, S., 2021. Carbon turnover times shape topsoil carbon difference between Tibetan Plateau and Arctic tundra. Science Bulletin 66, 1698–1704.
Wu, L., Wen, C., Qin, Y., Yin, H., Tu, Q., Van Nostrand, J.D., Yuan, T., Yuan, M., Deng, Y., Zhou, J., 2015. Phasing amplicon sequencing on Illumina Miseq for robust environmental microbial community analysis. BMC Microbiology 15, 125.
Yao, F., Yang, S., Wang, Z., Wang, X., Ye, J., Wang, X., DeBruyn, J.M., Feng, X., Jiang, Y., Li, H., 2017. Microbial taxa distribution is associated with ecological trophic cascades along an elevation gradient. Frontiers in Microbiology 8, 2071.
Yuan, M.M., Guo, X., Wu, L., Zhang, Y., Xiao, N., Ning, D., Shi, Z., Zhou, X., Wu, L., Yang, Y., Tiedje, J.M., Zhou, J., 2021. Climate warming enhances microbial network complexity and stability. Nature Climate Change 11, 343–348.
Zhou, J., Xue, K., Xie, J., Deng, Y., Wu, L., Cheng, X., Fei, S., Deng, S., He, Z., Van Nostrand, J.D., Luo, Y., 2012. Microbial mediation of carbon-cycle feedbacks to climate warming. Nature Climate Change 2, 106–110.
Zhu, J., Chen, N., Zhang, Y., Yaojie, L., 2016. Effects of experimental warming on net ecosystem CO2 exchange in Northern Xizang alpine meadow. Chin J Plant Ecol 40, 1219–1229.